LA-9683-MS

Los Alamos National Laboratory is operated by the University of California for the United States Department of Energy under contract W-7405-ENG-36.

DO NOT CIRCULATE

PERMANENT RETENTION

REQUIRED BY CONTRACT

LOS ALAMOS NATIONAL LABORATORY
3 9338 00308 7912

Energy Deposition from Particle Beams

Los Alamos National Laboratory
Los Alamos, New Mexico 87545

An Affirmative Action/Equal Opportunity Employer

This work was supported by the US Air Force Rocket Propulsion Laboratory, Edwards Air Force Base, California.

Prepared by Laurene Wolfe, Group WX-11

DISCLAIMER

This report was prepared as an account of work sponsored by an agency of the United States Government. Neither the United States Government nor any agency thereof, nor any of their employees, makes any warranty, express or implied, or assumes any legal liability or responsibility for the accuracy, completeness, or usefulness of any information, apparatus, product, or process disclosed, or represents that its use would not infringe privately owned rights. Reference herein to any specific commercial product, process, or service by trade name, trademark, manufacturer, or otherwise, does not necessarily constitute or imply its endorsement, recommendation, or favoring by the United States Government or any agency thereof. The views and opinions of authors expressed herein do not necessarily state or reflect those of the United States Government or any agency thereof.

LA-9683-MS

UC-34
Issued: November 1984

Energy Deposition from Particle Beams

W. Zack Osborne

LOS ALAMOS NATL. LAB. LIBS.
3 9338 00308 7912

Los Alamos National Laboratory
Los Alamos, New Mexico 87545

ENERGY DEPOSITION FROM PARTICLE BEAMS

by

W. Zack Osborne

ABSTRACT

A Fortran code named PARTEN, designed to compute electron or heavy-particle energy deposition in a layered, infinite plane target, has been written and tested by comparison with measurements. Ease of use, transportability, and economy in computing times were primary considerations.

I. INTRODUCTION

The program described in this report computes energy deposition from an electron beam or a heavy-particle (p, d, t, He, ...) beam in a layered, infinite plane target. The target may have as many as 50 layers of arbitrary thicknesses, and each layer may have up to 10 constituent elements. For heavy particles, energy deposition is almost entirely due to elastic interactions with target material electrons, but there are additional radiative energy-loss processes for e^- beams. In both cases, multiple scattering is primarily the result of elastic interactions with target material nuclei.

The user may choose to include or omit energy-loss straggling and multiple scattering detours. The user also has the option of including a treatment of the photon-electron multiplication and transport process for e^- beams.

II. HEAVY-PARTICLE BEAMS

We will consider first the simpler case in which straggling and multiple scattering are neglected. Barkas and Berger[1] give two empirical relations for proton ranges as functions of target atomic mass A and atomic number Z, of mean excitation energy for the target material, and of proton energy. These relations are:

for $1 \leq \tau \leq 9$ MeV (1)

$$\ln \lambda = -6.908 + \ln \frac{A}{Z} + \sum_{n=0}^{2} \sum_{m=0}^{2} a_{mn} (\ln I)^m (\ln \tau)^n , \tag{2}$$

and

for $9 < \tau \leq 1200$ MeV (3)

$$\ln \lambda = \ln \frac{A}{Z} + \sum_{n=0}^{3} \sum_{m=0}^{3} \alpha_{mn} (\ln I)^m (\ln \tau)^n . \tag{4}$$

In these equations,

λ = proton range in $g \cdot cm^{-2}$,

τ = proton kinetic energy in MeV,

I = mean excitation energy for target in eV, and

a_{mn}, α_{mn} = coefficients determined by least squares fits to experimental data.

Differentiation of these relations yields the stopping power formulas:

$$\frac{d\tau}{d\lambda} = \frac{\tau}{\lambda} \left[\sum_{n=1}^{2} \sum_{m=0}^{2} n a_{mn} (\ln I)^m (\ln \tau)^{n-1} \right]^{-1} \quad \frac{MeV}{g \cdot cm^{-2}} \tag{5}$$

and

$$\frac{d\tau}{d\lambda} = \frac{\tau}{\lambda} \left[\sum_{n=1}^{3} \sum_{m=0}^{3} n \alpha_{mn} (\ln I)^m (\ln \tau)^{n-1} \right]^{-1} \quad \frac{MeV}{g \cdot cm^{-2}} . \tag{6}$$

For elements, the mean excitation energies are obtained from the tabulated values given by Anderson and Ziegler.[2] If the target material has several constituent elements, the proton range is given by

$$\frac{1}{\lambda} = \sum_{i=1}^{n} \frac{f_i}{\lambda_i} , \tag{7}$$

where λ_i is the calculated range in the i^{th} constituent and f_i is the fraction by weight of that constituent.

Ranges for other heavy particles are related to proton ranges by

$$R(\beta) = \frac{M}{z^2} \left[\lambda(\beta) + B_z(\beta) \right] , \tag{8}$$

where β is velocity in units of light speed, M and z are particle mass and charge in units of proton mass and charge, and B_z is the range extension resulting from electron capture on the positively charged projectile as it traverses the target material. B_z is given by

$$B_z(I,\beta) = \left(48.0 + 5.8\ I^{5/8}\right) \frac{A}{Z} \times 10^{-5}\ \beta\ z^{5/3}\ g \cdot cm^{-2} \tag{9}$$

for $\beta < 2z/137$, and

$$B_z(I) = \left(7.0 + 0.85\ I^{5/8}\right) \frac{A}{Z} \times 10^{-6}\ z^{8/3}\ g \cdot cm^{-2} \tag{10}$$

for $\beta > 2z/137$. If there are several constituent elements, the individual R_i's are computed, and then R is obtained by

$$\frac{1}{R} = \sum_{i=1}^{n} \frac{f_i}{R_i} . \tag{11}$$

Proton stopping powers for single elements are computed with the appropriate formula of the pair exhibited earlier. For several constituents, the total stopping power is the sum of contributions from the individual elements

$$\frac{d\tau(\beta)}{d\lambda} = \sum_{i=1}^{n} f_i \frac{d\tau(\beta)}{d\lambda_i} . \tag{12}$$

Stopping powers for other heavy particles are given by

$$\frac{dT(\beta)}{dR} = z^{*2} \frac{d\tau(\beta)}{d\lambda} , \tag{13}$$

where z^* is the effective charge[3]

$$z^* = z\left[1 - \exp\left(-125\ \beta\ z^{-2/3}\right)\right], \tag{14}$$

and $T(\beta)$ is the heavy-particle kinetic energy at velocity β.

Nuclear interactions of heavy particles have been ignored. Some brief quantitative considerations illustrate the range of validity of this neglect. A nominal (geometric) mean free path for protons is 100 $g \cdot cm^{-2}$ or 37 cm in aluminum. Representative mean free paths for some heavier projectiles are 10 $g \cdot cm^{-2}$ for iron and 3 $g \cdot cm^{-2}$ for uranium. It is roughly true that heavy particle ranges of one mean free path correspond to energies of 400 MeV/nucleon. Tritons and deuterons are exceptions because M/z^2 is, respectively, 3 and 2 for these projectiles.

It may sometimes be desirable to invert the empirical range-energy relationship. Because range is a monotonically increasing function of energy, the proton energy and velocity corresponding to a given range can be found to suitable accuracy by successive approximations in which trial energies are obtained by sequentially halving intervals.

Inclusion of straggling and multiple scattering is most readily accomplished by Monte Carlo methods. A random number generator is used to select track quantities from relevant distributions for each member of a set of test particles. Energy deposits are then accumulated in an appropriate set of $\Delta\ell$ intervals, where ℓ is measured in a direction normal to the target interfaces.

Given an initial kinetic energy T_1 for a heavy-particle beam, it is easy to find the corresponding velocity β_1 and equivalent proton kinetic energy τ_1. Next, a set of τ_j's is defined by equal intervals in $\ln\tau$.

τ_1 = equivalent proton kinetic energy at target entrance,

$$\tau_2 = \exp\left(\frac{n-1}{n} \ln \tau_1\right), \tag{15}$$

$$\tau_3 = \exp\left(\frac{n-2}{n} \ln \tau_1\right), \text{ and} \qquad (16)$$
$$\tau_{n+1} = 1 \text{ MeV} .$$

For a particular Monte Carlo particle, the calculation proceeds in the following manner. Begin at the target entrance and compute

$$\lambda(\tau_1),\ R(\beta_1),\ S(\beta_1),\ T(\beta_1),$$
$$\lambda(\tau_2),\ R(\beta_2),\ S(\beta_2),\ T(\beta_2),$$

where $S^2(\beta_j)$ is the variance in $R(\beta_j)$ as a result of straggling. $\sigma^2(\beta_j)$ is the corresponding variance in $\lambda(\beta_j)$. S and σ are related by[4]

$$S(\beta) = \frac{R(\beta)}{\lambda(\beta)\sqrt{M}}\,\sigma(\beta). \qquad (17)$$

$\sigma(\beta_j)$ is obtained by interpolation within a table[5] of σ's vs proton energy and mean excitation energy. A value of ΔR is chosen randomly from the Gaussian distribution

$$\exp\left[-\frac{(\Delta R - \overline{\Delta R})^2}{2\,s^2}\right], \qquad (18)$$

where $\overline{\Delta R} = R_j - R_{j+1}$ and $s^2 = S_j^2 - S_{j+1}^2$.

The following steps are then executed.

Compute $\Delta\ell$ from ΔR and the trajectory at entrance into ΔR.

Does $\Delta\ell$ extend across a target interface?

No → proceed to multiple scattering calculation.

Yes → is this the last (that is, exit) interface?

If so, add energy deposits to $\Delta\ell$ bins in the last layer and start over with a new Monte Carlo test particle. If not, do the following:

Get τ(Interface) by interpolation and then get β(Interface) and T(Interface).

Get λ(Interface, next material).

Get R(Interface, next material).

Get S(Interface, next material).

Shorten the last $\Delta\ell$ so that the end point coincides with interface and adjust last ΔR accordingly.

Go to multiple scattering calculation.

The multiple scattering calculation starts with the random selection of a scattering angle from the Gaussian distribution[6]

$$\exp\left(-\frac{\theta^2}{2\langle\theta^2\rangle}\right), \tag{19}$$

where

$$\langle\theta^2\rangle = z^2\left(\frac{21}{p\beta}\right)^2 \frac{\Delta R}{X}, \quad p \geq 125\ Z^{-1/3} \tag{20}$$

and

$$\langle\theta^2\rangle = z^2 \frac{\ln\left(267.9\ Z^{-1/3}\ p\right)}{2\ \ln\left(183\ Z^{-1/3}\right)}\left(\frac{21}{p\beta}\right)^2 \frac{\Delta R}{X}, \quad p < 125\ Z^{-1/3}. \tag{21}$$

p is projectile momentum in MeV/c and X is radiation length for the target material. Finally, the polar scattering angle θ and a randomly chosen azimuthal angle are used to alter the test particle trajectory upon exit from ΔR.

The calculation continues through the established steps in τ until the test particle either stops or exits the target.

III. ELECTRON BEAMS

As before, we will discuss first the option under which straggling and multiple scattering are not included. Two choices are still possible--ignore photon-electron multiplication and transport or carry out an evaluation of these processes.

Both energy-loss straggling (primarily in radiative interactions) and multiple scattering are important effects for energetic electron beams, but mean energy-loss rates and mean ranges are informative even when strong fluctuations are present.

Berger and Seltzer[7] have prepared extensive tables of mean energy-loss rates and ranges as functions of electron energy in many different materials. For our purposes, these tables can be abridged to reasonable size for storage in memory without unduly degrading accuracy.

Interpolation within these abridged tables yields $\left(\frac{dE}{dR}\right)_{total}$ vs E (E is electron kinetic energy) and R vs E. The nonradiative portion $\left(\frac{dE}{dR}\right)_{coll}$ of the energy loss rate can be obtained from analytic expressions quoted by Berger and Selzer.[7] This approach incorporates the density effect correction resulting from polarization of the target medium. With these ingredients, obtaining both $\left(\frac{dE}{dR}\right)_{total}$ and $\left(\frac{dE}{dR}\right)_{coll}$ as functions of location in the target is straightforward. For target thicknesses somewhat less than a radiation length, most of the radiated energy escapes from the target, and mean energy deposition is described adequately by $\left(\frac{dE}{dR}\right)_{coll}$ as a function of location in the target. The collision energy-loss rate for an electron in a one-element target is

$$-\left(\frac{dE}{dR}\right)_{coll} = \frac{2\pi N r_o^2 mc^2}{\beta^2}\frac{Z}{A}\left\{\ln\left[\frac{t^2(t+2)}{2\left(I/mc^2\right)^2}\right] + F(t) - \delta\right\}. \tag{22}$$

In this equation,

$F(t) = 1 - \beta^2 + [t^2/8 - (2t+1)\ln 2]/(t+1)^2$,

mc^2 = electron rest energy = 0.511 MeV,

t = electron kinetic energy in units of mc^2,

β = electron velocity in units of the speed of light,

Z = atomic number for target,

A = atomic weight for target,

δ = density effect correction,

N = Avogadro's number = 6.02×10^{23}, and

r_o = classical radius of electron = 2.82×10^{-13} cm, and the energy loss rate is expressed in MeV/g·cm^{-2}. The density effect correction is given by

$$\delta = \begin{cases} 0, & y < y_o \\ \ln\left[\beta^2/\left(1-\beta^2\right)\right] + C + a\,(y_1 - y)^m, & y_o \le y < y_1, \\ \ln\left[\beta^2/\left(1-\beta^2\right)\right] + C, & y \ge y_1 \end{cases} \tag{23}$$

where

$$y = 0.217 \ln\left[\beta^2/\left(1-\beta^2\right)\right].$$

y_0, y_1, C, a, and m are parameters that depend on target identity, and that are evaluated as recommended by Sternheimer.[8]

Inclusion of straggling and multiple scattering for primaries without showers requires a Monte Carlo calculation. An appropriate set of $\Delta\ell$'s is set up, and propagation of each primary electron is initiated at the target entrance. Because of multiple scattering, the trajectory will change from interval to interval, and straggling will cause fluctuations in energy loss even in equal path lengths at the same primary energy. The ΔR corresponding to each $\Delta\ell$ is obtained from the entrance (into $\Delta\ell$) trajectory and $\Delta\ell$ itself. The entrance energy is known from previous calculations so $\left(\frac{dE}{dR}\right)_{coll}$ can be obtained exactly as before. The energy lost in traversal of ΔR is selected randomly from an analytic distribution given by Eyges.[9] To within a normalization constant, the Eyges distribution is

$$\left(\frac{E}{E_0-\varepsilon}\right)^{0.25} \left[\ln\left(\frac{E_0-\varepsilon}{E}\right)\right]^{\Delta r-1} , \tag{24}$$

where

E_0 = electron kinetic energy at beginning of ΔR,

$\Delta r = 4\Delta R/(3X)$,

X = target radiation length,

E = randomly selected energy after traversal of ΔR, and

ε = ionization energy loss during traversal of ΔR.

If the target is composed of several constituent elements, the radiation length is

$$\frac{1}{X} = \sum_{i=1}^{n} \frac{f_i}{X_i} . \tag{25}$$

This procedure assumes all straggling is due to radiative interactions, but it includes mean energy loss from elastic collisions. [Alteration of the trajectory at exit from ΔR because of multiple scattering is done in the same manner as it was for heavy particles.] The program steps through $\Delta\ell$'s until the primary electron stops or exits the target. Enough test electrons are cycled through to assure adequate statistics.

Energy deposition can also be computed for the case in which straggling and showers are ignored, but multiple scattering and mean energy loss rates are incorporated.

If the target is thicker than one radiation length (representative values are Be--35 cm, C--19 cm, Al--9 cm, Fe--1.8 cm, Ag--0.9 cm, and U--0.3 cm), then a significant portion of the energy deposition takes place through photon-electron transport and multiplication. A Monte Carlo calculation is used to evaluate these processes. We assume that contributions from Compton scattering and from the photoelectric effect can be neglected, as compared with contributions from pair production. Positron-electron annihilation into two or three photons is also ignored, and all reactions are taken to be collinear. The probability of producing a bremsstrahlung photon in an electron path length ΔR is

$$P_\gamma\left(\frac{\Delta R}{X}\right), \tag{26}$$

where X is radiation length and $\Delta R \ll X$. P_γ is weakly dependent on primary energy and is obtained from a fit to integrals of spectra given by Rossi.[6] If a photon is produced, it is assigned an energy by sampling an empirical distribution that depends on primary energy and represents Rossi's[6] spectra. The probability of pair production by a photon in path length ΔR is

$$P_p\left(\frac{\Delta R}{X}\right), \tag{27}$$

where P_p depends on photon energy and weakly on target average atomic number. The photon energy dependence is contained in a simple analytical fit to a curve given by Rossi,[6] and a weak linear dependence on average atomic number is chosen by comparisons of computer results with measured data. The energy of one member of the pair is selected from a flat distribution between kinematic minimum and maximum, and the energy of the other member of the pair is then chosen to conserve total energy.

As a prelude to iteration through a set of Monte Carlo test electrons, a sequence of $\Delta\ell$'s is set up so that a boundary coincides with each target interface. Every primary test electron propagates either to the end of its range or entirely through the target,

depositing ionization energy in $\Delta\ell$ bins along its path at the user's option. As each test electron is propagated, a memory stack of secondary photons is accumulated. After propagation of the primary test electron is completed, the calculation steps through the photon stack and accumulates a memory stack of secondary e^+ and e^- from pair production. Each secondary and higher generation $e^\pm$ is propagated in the same manner as a primary electron, and a photon stack is accumulated. This process is continued to the logical end dictated by either a photon energy cutoff (lower limit) of 10 MeV or the emptying of photon and $e^\pm$ stacks. We ignore the small differences in energy-loss rates for electrons and positrons. The user may choose to include or neglect multiple scattering of primary and higher generation electrons in the shower simulations. If included, the multiple scattering effects are computed in exactly the same manner as in the heavy-particle case.

User options are listed in Appendix A, comparisons of calculations with measurements are shown in Appendix B, common block definitions are given in Appendix C, and Appendix D contains subroutine descriptions.

APPENDIX A

USER OPTIONS

The user has the following options for heavy particles:

1. Ignore straggling and multiple scattering.
2. Include both straggling and multiple scattering.
3. In Monte Carlo calculations, the user specifies the number of histories.

The options listed below are available for electrons.

1. Compute nominal (mean) energy deposition for beam particles alone with no straggling or multiple scattering.
2. Compute nominal deposition for beam particles with multiple scattering but no straggling. This is a Monte Carlo calculation.
3. Compute deposition for beam particles with both multiple scattering and straggling (from Eyges distribution) included. This is a Monte Carlo calculation.
4. Compute deposition with both showers and multiple scattering included. This is a Monte Carlo calculation.
5. In calculations with showers, deposition from primaries may be included or omitted.

APPENDIX B

COMPARISONS

Run times are less than 10 min. (CDC 7600) for 20% statistics and the most complex target structure possible.

Comparisons with the following measurements are illustrated in Figs. B-1 through B-8.

338.5 MeV protons in Pb 338.5 MeV protons in Cu	Mather and Segre, Phys. Rev. 84, 191 (1951).
1000 MeV electrons in Al 1000 MeV electrons in H_2O	Crannell and Crannell, Phys. Rev. 184, 426 (1969).
900 MeV electrons in Pb 900 MeV electrons in Sn 900 MeV electrons in Cu 200 MeV electrons in Pb	C. J. Crannell, Phys. Rev. 161, 310 (1967).

Comparisons with more elaborate Monte Carlo calculations of Berger and Seltzer are shown in Figs. B-9 and B-10.

60 MeV electrons in W
30 MeV electrons in W

Berger and Seltzer, Phys. Rev. 2C, 621 (1970).

APPENDIX C

COMMON BLOCK DEFINITIONS

I. /TARG/ZT(50,10), AT(50,10), RHO(50,10), NEL(50), DXL(50), LAY, EIM(50), DL(50), DEN(50), DTOT, X(50), XX(50,10), ZBAR(50)

This block contains the following input and calculated target data:

ZT(J,I) = atomic number for I^{th} element in J^{th} layer.
AT(J,I) = atomic weight for I^{th} element in J^{th} layer.
RHO(J,I) = density in $g \cdot cm^{-3}$ for I^{th} element in J^{th} layer.
NEL(J) = number of elements in J^{th} layer.
DXL(J) = thickness of J^{th} layer in $g \cdot cm^{-2}$.
LAY = number of layers.
EIM(J) = average excitation energy for J^{th} layer.
DL(J) = energy deposition bin size in $g \cdot cm^{-2}$ for the J^{th} layer.
DEN(J) = total density for J^{th} layer.
DTOT = total target thickness in $g \cdot cm^{-2}$.
X(J) = average radiation length for J^{th} layer in $g \cdot cm^{-2}$.
XX(J,I) = radiation length in $g \cdot cm^{-2}$ for I^{th} element of J^{th} layer.
ZBAR(J) = average atomic number for J^{th} layer.

ZT, AT, RHO, NEL, DXL, and LAY are input data. EIM is calculated in subroutine EIMIX; X and XX in GETX; DL, DEN, DTOT, and ZBAR in FIXINT.

II. /DEPOS/ED(2000), INLA(51), XMID(2000), NBN, EPERC(2000), TSV(2000).

This block contains energy deposition results and bin specifications.

ED(N) = energy deposition rate in MeV/g·cm^{-2} for Nth bin. N = 1 corresponds to beam entrance surface.

INLA(J) = index (N) of first bin in Jth layer.

XMID(N) = coordinate (in cm) of midpoint of Nth bin. Entrance surface is at XMID = 0.0.

NBN = total number of bins.

EPERC(N) = energy deposition rate in MeV/cm for Nth bin.

TSV(N) = kinetic energy of particle at entrance into Nth bin--for some options.

III. /EPLST/NECR(1000), TECR(1000), CTE(1000), SPE(1000), CPE(1000), NPH(1000), EPH(1000), CTP(1000), SPP(1000), CPP(1000) IEMX, IPMX

This block contains information about electrons and photons in Monte Carlo showers.

NECR(L) = bin index for origin of Lth electron in a given generation.

TECR(L) = kinetic energy in MeV for Lth electron in a given generation at its origin.

CTE(L) = $\cos\theta$ for Lth electron at its origin, where polar axis is initial beam direction.

SPE(L) = $\sin\phi$ for Lth electron at its origin, where ϕ is azimuthal angle in plane perpendicular to beam axis.

CPE(L) = $\cos\phi$ for Lth electron at its origin.

NPH(L) = bin index for origin of Lth photon in a given generation.

EPH(L) = energy in MeV for Lth photon.

CTP(L) = $\cos\theta$ for Lth photon.

SPP(L) = $\sin\phi$ for Lth photon.

CPP(L) = $\cos\phi$ for Lth photon.

IEMX = number of $e^{\pm}$ in a given generation.

IPMX = number of photons in a given generation.

APPENDIX D

SUBROUTINE DEFINITIONS

I. HEVA (CP, PRMS, TI)

This subroutine computes energy deposition for heavy particles (CP = charge and PRMS = mass, both in proton units) with initial kinetic energy TI. Both straggling and multiple scattering are ignored. TI is expressed in MeV and energy deposition is given both in $MeV/g \cdot cm^{-2}$ and MeV/cm as functions of location in the target. The routine uses common blocks TARG and DEPOS. DEPOS arrays ED(N) and EPERC(N) contain energy deposition results. Array TSV(N) contains the particle energy at entrance into each depth interval.

II. FIXINT (NIN)

This subroutine initializes common block DEPOS and sets up NIN energy deposition bins. It computes DL(J), DEN(J), DTOT, ZBAR(J), INLA(J), and XMID(N). Common blocks TARG and DEPOS are used by the routine.

III. ENOM (TI, NZ, NLAST)

This subroutine computes mean ionization energy deposition for electrons with initial kinetic energy TI (in MeV) that originate in bin number NZ. Straggling and multiple scattering are neglected and no electromagnetic shower calculation is included. The computation ends with bin number NLAST, and the routine returns TI, the energy at exit from the last bin. Common blocks TARG and DEPOS are used by the routine. Arrays ED(N) and EPERC(N) in DEPOS contain the energy deposition results. Array TSV(N) contains the electron energy at entrance into each bin.

IV. GETX

This subroutine computes XX(J,I), the radiation lengths for the various elements, and X(J), the average radiation length for each layer. It uses common block TARG.

V. ESHOW (TI, NMC, IBR)

This subroutine computes electron beam energy deposition as a function of depth in the target with electromagnetic showers evaluated. Multiple scattering is ignored, but radiative straggling is implicit in the Monte Carlo process. The calculation iterates through NMC Monte Carlo primaries, each with initial kinetic energy TI in MeV. If IBR > 0, only secondary and later generation electrons deposit energy. If IBR = 0, primary and later generation electrons deposit energy. The routine uses common blocks EPLST, DEPOS, and TARG. DEPOS arrays ED(N) and EPERC(N) contain the energy deposition results, and XMID(N) contains the corresponding target depths in cm.

VI. ENMASC (TI, NZ, NLAST, CTZ, SPZ, CPZ)

This subroutine computes mean ionization energy deposition for electrons with initial kinetic energy TI that originate in bin number NZ. Multiple scattering is included, but straggling and showers are ignored. The initial trajectory is defined by $\cos\theta$ = CTZ, $\sin\phi$ = SPZ, and $\cos\phi$ = CPZ. The computation ends with bin number NLAST. The routine returns TI, the energy at exit from the last bin, and CTZ, SPZ, CPZ = $\cos\theta$, $\sin\phi$, $\cos\phi$ at exit from the last bin. This routine uses common blocks DEPOS and TARG. DEPOS arrays ED(N) and EPERC(N) contain the energy deposition results.

VII. ESTASC (TI, NZ, NLAST, CTZ, SPZ, CPZ)

This subroutine computes ionization energy deposition for electrons with initial kinetic energy TI that originate in bin number NZ. Both straggling (radiative) and multiple scattering are included, but showers are ignored. The initial trajectory is defined by $\cos\theta$ = CTZ, $\sin\phi$ = SPZ, and $\cos\phi$ = CPZ. The computation ends with bin number NLAST. The routine returns TI = energy and CTZ, SPZ, CPZ = $\cos\theta$, $\sin\phi$, $\cos\phi$ at exit from the last bin. It uses common blocks DEPOS and TARG. DEPOS arrays ED(N) and EPERC(N) contain the energy deposition results.

VIII. ESCASH (TI, NMC, IBR)

This subroutine computes electron beam energy deposition as a function of depth in the target with electromagnetic showers evaluated. Multiple scattering is included and radiative straggling is implicit in the Monte Carlo process. The calculation iterates through NMC Monte Carlo primaries, each with initial kinetic energy TI in MeV. If IBR > 0, only secondary and later generation electrons deposit energy. If IBR = 0, primary and later generation electrons deposit energy. The routine uses common blocks EPLST, DEPOS, and TARG. DEPOS arrays ED(N) and EPERC(N) contain the energy deposition results, and XMID(N) contains the corresponding target depths in cm.

IX. BREM (C, T)

This subroutine computes a material-independent multiplier that is used in assigning a probability for bremsstrahlung. The multiplier C is obtained by interpolation between values from integrals of curves given by Rossi for several primary electron energies. T is the primary electron kinetic energy in MeV.

X. EBREM (TP, T)

This subroutine selects an energy for a bremsstrahlung photon by interpolation between linear fits to curves given by Rossi[6] for various primary energies. TP is the selected photon energy in MeV, and T is the primary electron kinetic energy.

XI. HSTASC (ZP, PRMS, TI, NMC)

This subroutine computes energy deposition for heavy particles (ZP = charge and PRMS = mass, both in proton units) with initial kinetic energy TI in MeV. Multiple scattering and straggling are both included. Energy deposition is given in MeV/g•cm^{-2} and in MeV/cm as functions of depth in the target. NMC specifies the number of Monte Carlo test particles. The routine uses common blocks DEPOS and TARG. DEPOS arrays ED(N) and EPERC(N) contain the energy deposition results, and XMID(N) contains the corresponding target depths in cm.

XII. RHEVY (RH, RP, CP, PRMS, V, EXAV, ATW, CT)

This subroutine computes range for a heavy particle in a target that is a pure element.

RH = heavy-particle range returned by routine.
RP = range of a proton with the same velocity. This is input for the routine and is obtained from RPRO.
CP = heavy-particle charge in proton units.
PRMS = heavy-particle mass in proton units.
V = speed in units of speed of light.
EXAV = average excitation energy for target in eV.
ATW = atomic weight for target.
CT = atomic number for target.

Ranges are expressed in g•cm^{-2}.

XIII. SUMIN (X, F, Y, NEL)

This subroutine computes range in a target consisting of as many as 10 elements from ranges in the individual elements.

$X = \left[\sum F_i/Y_i\right]^{-1}$ = target range in $g \cdot cm^{-2}$.

F_i = fraction by weight of i^{th} element.

Y_i = range in i^{th} element in $g \cdot cm^{-2}$.

XIV. EFCH (Z, ZZ, B)

This subroutine computes effective charge for a heavy particle with given speed and bare charge.

Z = effective charge returned by routine.
ZZ = bare charge for heavy particle in proton units.
B = particle speed in units of light speed.

XV. WTSUM (X, F, Y, NEL)

This subroutine computes the weighted sum of stopping powers for a target consisting of as many as 10 elements.

$X = \sum F_i Y_i$ returned by routine.
F_i = fraction by weight of i^{th} element.
Y_i = stopping power in $MeV/g \cdot cm^{-2}$ for i^{th} element.

XVI. RPRO (R, S, T, EX, ATW, CT, IBR)

This subroutine computes range and (optionally) stopping power for a proton of given kinetic energy in a target that consists of only one element.

R = proton range (in $g \cdot cm^{-2}$) returned by the routine.

S = proton stopping power (ionization energy loss rate in $MeV/g \cdot cm^{-2}$) returned by the routine.

T = proton kinetic energy in MeV.

EX = average excitation energy (in eV) for the target.

ATW = atomic weight for the target.

CT = atomic number for the target.

IBR = branching specifier. If IBR < 1, compute only R. If IBR $\geq$ 1, compute both R and S.

XVII. AVEX (EX, Z)

This subroutine computes the average excitation energy EX (in eV) for an elemental target with atomic number Z.

XVIII. SCOL (S, T, ATW, CT, EX)

This subroutine computes the ionization energy-loss rate for an electron beam in an elemental target.

S = ionization energy-loss rate in $MeV/g \cdot cm^{-2}$ returned by the routine.

T = electron kinetic energy in MeV.

ATW = atomic weight for the target.

CT = atomic number for the target.

EX = average excitation energy in eV for the target.

XIX. STOT (ST, T, Z, RM)

This subroutine computes the mean total (radiative plus ionization) energy-loss rate and mean range for an electron beam in an elemental target.

ST = total energy loss rate in $MeV/g \cdot cm^{-2}$ returned by the routine.

T = electron kinetic energy in MeV.

Z = atomic number for the target.
RM = mean electron range in $g \cdot cm^{-2}$ returned by the routine.

XX. STRAG (S, RH, VM, TX, EX)

This subroutine computes the standard deviation of the range distribution for a heavy particle.

S = standard deviation of the range returned by the routine.
RH = mean range for the heavy particle.
VM = heavy-particle mass in proton units.
TX = kinetic energy of a proton with the same speed as the heavy particle.
EX = average excitation energy (in eV) for the target.

XXI. EIMIX

This subroutine computes the average excitation energy for a target consisting of a mixture of several (as many as 10) elements. It uses common block TARG, and the average excitation energies are stored in array EIM(J).

XXII. DELR (R, RB, SSQ)

This subroutine selects a Monte Carlo range from a Gaussian distribution with specified variance and mean range.

R = selected range returned by the routine.
RB = mean range.
SSQ = variance for the range distribution.

As applied here, RB is the difference in ranges for two different energies, and SSQ is the variance for the range difference.

XXIII. SCAT (TH, Z, P, B, R, X, ZT)

This subroutine selects a Monte Carlo multiple scattering angle from a Gaussian distribution with variance appropriate to the specified projectile and target properties.

TH = selected scattering angle returned by the routine (radians).
Z = projectile charge in proton units.
P = projectile momentum in MeV/c.
B = projectile speed in units of the speed of light.
R = range interval over which the multiple scattering occurs ($g \cdot cm^{-2}$).
X = (mean) radiation length for the target ($g \cdot cm^{-2}$).
ZT = (mean) atomic number for the target.

XXIV. EYGES (E, EZ, EC, R, X)

This subroutine selects a Monte Carlo energy from the Eyges analytic distribution to include radiative straggling for electrons.

E = kinetic energy remaining after traversal of specified range interval.
EZ = initial kinetic energy.
EC = ionization energy deposited by electron during traversal of range interval.
R = range interval in $g \cdot cm^{-2}$.
X = (mean) radiation length for target in $g \cdot cm^{-2}$.
All energies are in MeV.

XXV. RADL (X, Z)

This subroutine selects and returns the radiation length (in $g \cdot cm^{-2}$) for an element with atomic number Z.

XXVI. EPRO (R, E, EMAX, EI, ATW, CT)

This subroutine iteratively computes the proton kinetic energy (in MeV) corresponding to a given proton range ($g \cdot cm^{-2}$) in a specified elemental target.

R = proton range.
E = proton kinetic energy returned by the routine.
EMAX = energy upper limit given as input.
EI = average excitation energy (in eV) for the target.
ATW = atomic weight for the target.
CT = atomic number for the target.

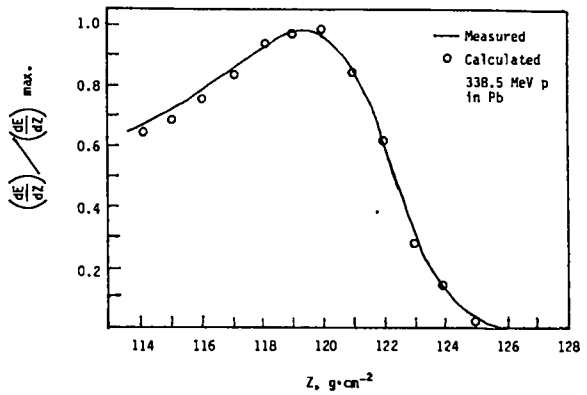

Fig. B-1.

Comparison of measured and calculated energy deposition rates versus depth for protons of initial energy 338.5 MeV in lead.

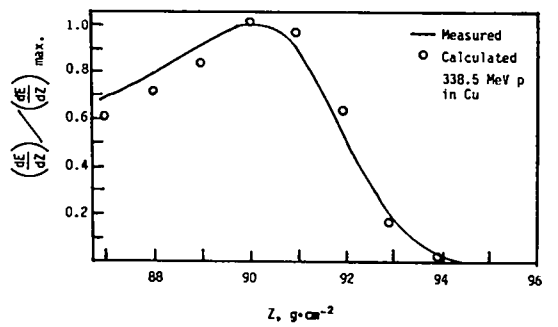

Fig. B-2.

Comparison of measured and calculated energy deposition rates versus depth for protons of initial energy 338.5 MeV in copper.

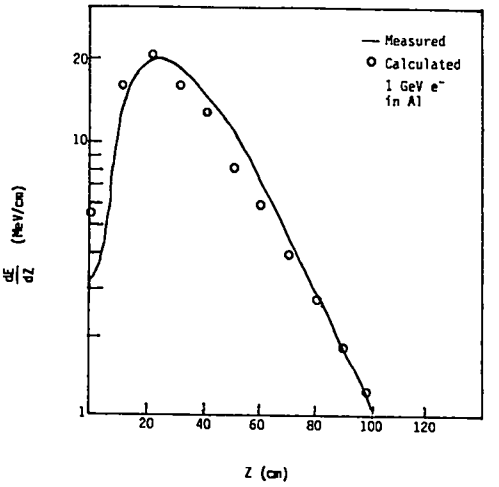

Fig. B-3.

Comparison of measured and calculated energy deposition rates versus depth for electrons of initial energy 1 GeV in aluminum.

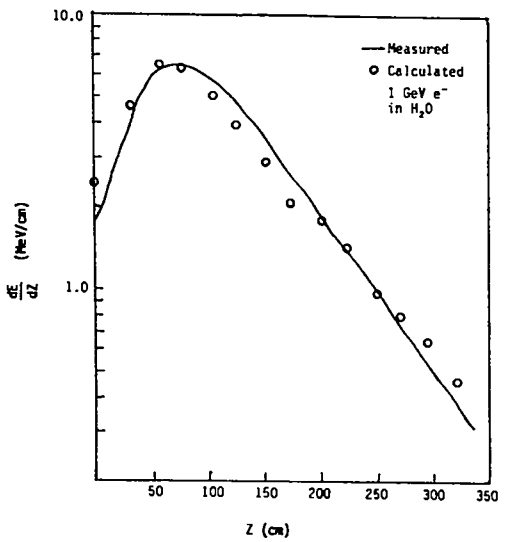

Fig. B-4.

Comparison of measured and calculated energy deposition rates versus depth for electrons of initial energy 1 GeV in water.

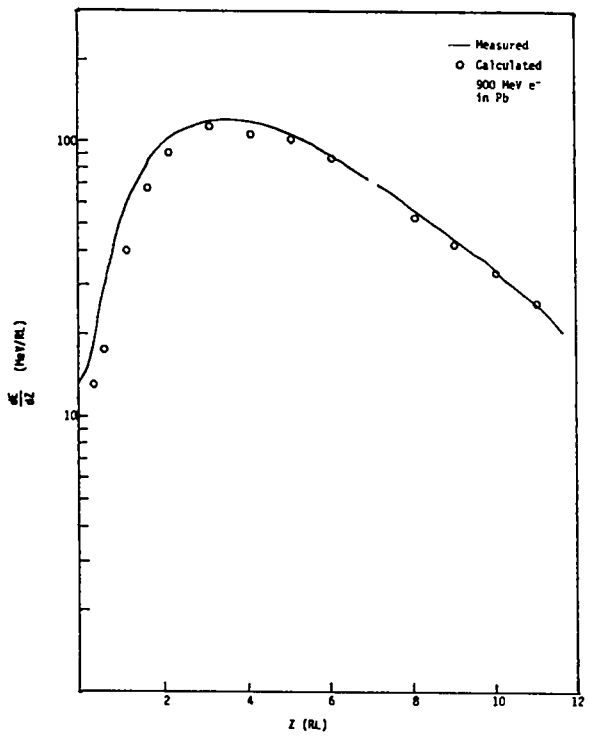

Fig. B-5.

Comparison of measured and calculated energy deposition rates versus depth for electrons of initial energy 900 MeV in lead. RL is radiation length.

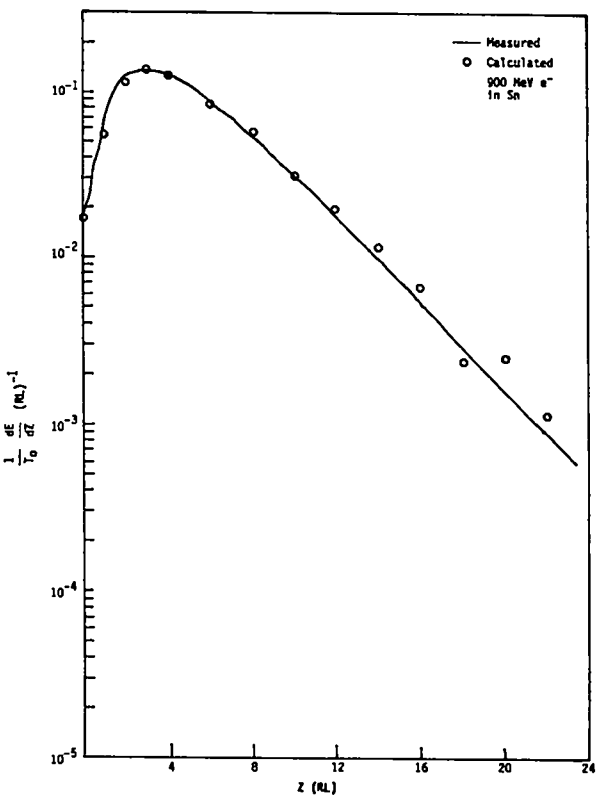

Fig. B-6.

Comparison of measured and calculated energy deposition rates versus depth for electrons of initial energy 900 MeV in tin. RL is radiation length and T_o is electron initial kinetic energy.

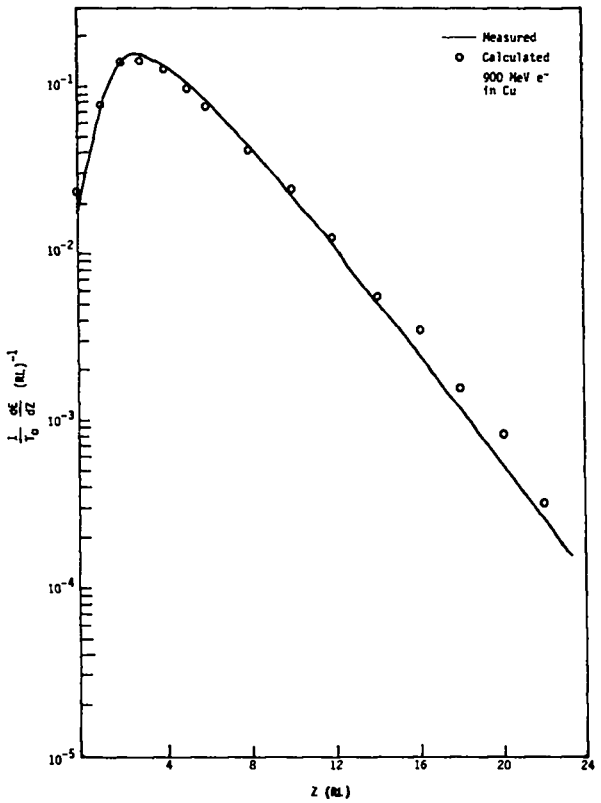

Fig. B-7.

Comparison of measured and calculated energy deposition rates versus depth for electrons of initial energy 900 MeV in copper. RL is radiation length and T_0 is electron initial kinetic energy.

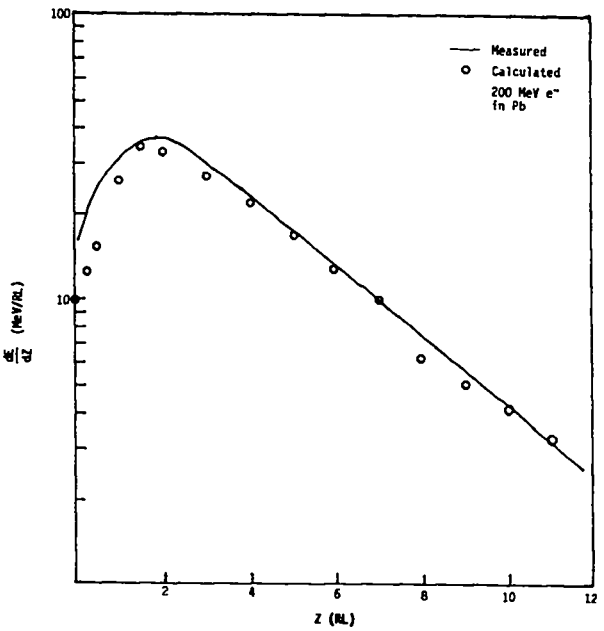

Fig. B-8.

Comparison of measured and calculated energy deposition rates versus depth for electrons of initial energy 200 MeV in lead. RL is radiation length.

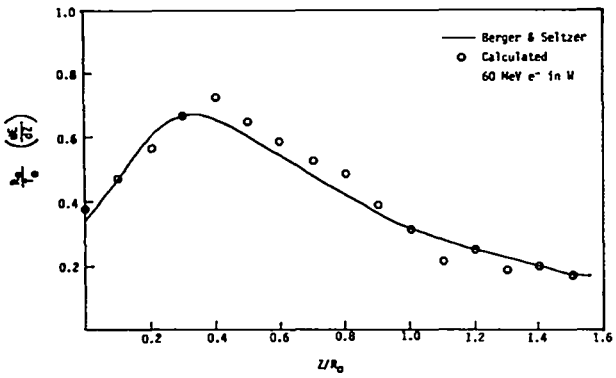

Fig. B-9.

Comparison of calculated energy deposition rate versus depth and the elaborate Monte Carlo computation of Berger and Seltzer for electrons of initial energy 60 MeV in tungsten. R_0 is the nominal electron range and T_0 is electron initial kinetic energy.

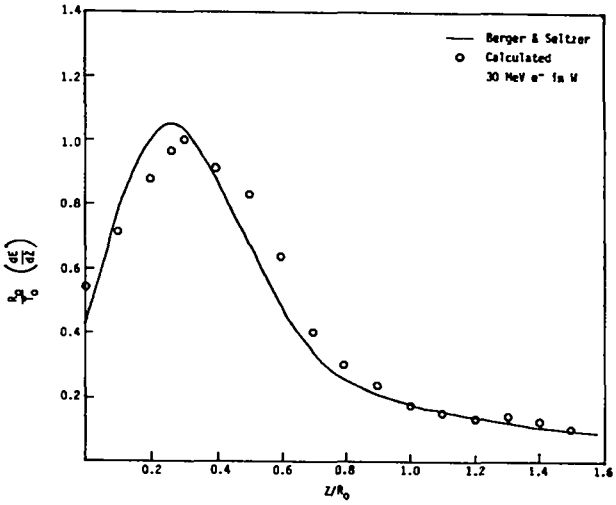

Fig. B-10.

Comparison of calculated energy deposition rate versus depth and the computation of Berger and Seltzer for electrons of initial kinetic energy 30 MeV in tungsten. T_0 is electron initial kinetic energy and R_0 is the nominal electron range.

REFERENCES

1. W. H. Barkas and M. J. Berger, "Studies in Penetration of Charged Particles in Matter," U. Fano, Ed., National Academy of Sciences and National Research Council publication 1133, report no. 7 (1964).

2. H. H. Anderson and J. F. Ziegler, The Stopping and Ranges of Ions in Matter, Vol. III (Pergamon Press, New York, 1977).

3. W. H. Barkas, Nuclear Research Emulsions, Vol. I (Academic Press, New York, 1963), p. 371.

4. W. H. Barkas, Nuclear Research Emulsions, Vol. II (Academic Press, New York, 1973), p. 53.

5. R. M. Sternheimer, Phys. Rev. 117, 485 (1960).

6. B. Rossi, High Energy Particles, (Prentice Hall, New York, 1952), pp. 66-77.

7. M. J. Berger and S. M. Seltzer, "Studies in Penetration of Charged Particles in Matter," U. Fano, Ed., National Academy of Sciences and National Research Council publication 1133, report no. 10 (1964).

8. R. M. Sternheimer, Phys. Rev. 103, 511 (1956).

9. L. Eyges, Phys. Rev. 76, 264 (1949).

Printed in the United States of America
Available from
National Technical Information Service
US Department of Commerce
5285 Port Royal Road
Springfield, VA 22161

Microfiche (A01)

Page Range	NTIS Price Code
001-025	A02
026-050	A03
051-075	A04
076-100	A05
101-125	A06
126-150	A07
151-175	A08
176-200	A09
201-225	A10
226-250	A11
251-275	A12
276-300	A13
301-325	A14
326-350	A15
351-375	A16
376-400	A17
401-425	A18
426-450	A19
451-475	A20
476-500	A21
501-525	A22
526-550	A23
551-575	A24
576-600	A25
601-up*	A99

*Contact NTIS for a price quote.

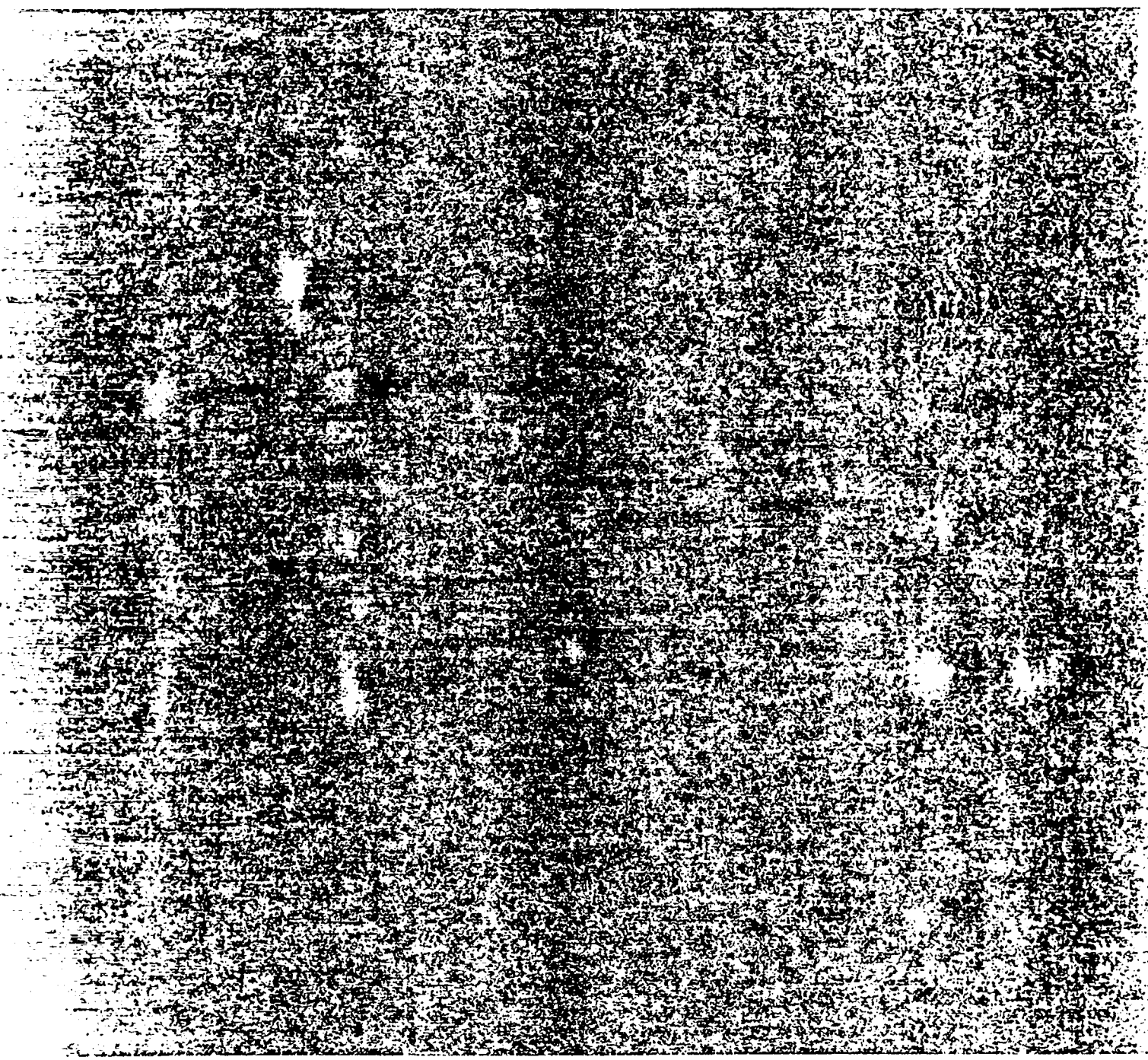

Los Alamos